Chapter 1

Introduction

1.1 Overview

Computer simulations have become a universal and indispensable tool in many fields of physics and chemistry, including materials science. The effort to design, characterize, and optimize materials properties using computer simulations integrates various computational methods, such as quantum mechanics (QM), molecular dynamics (MD), and finite element methods (FEM). In particular, MD in connection with statistical mechanics can provide useful thermodynamic and kinetic data as well as theoretical insights into complex systems.

Among complex systems, glasses have been vigorously studied both experimentally and computationally, yet they are not completely understood. The glass transition has been cited as one of the major unsolved problems in solid state physics (Anderson, 1995). Theoretically, the simplest systems are metallic glasses because of their highly symmetric building blocks (atoms) and isotropic interactions (metallic bonding). In this thesis, we use MD to investigate phase behavior and related thermodynamic as well as, structural, and mechanical properties of metals and alloys in both crystalline and glass states. In addition, QM is incorporated with MD to describe properties of some realistic systems, such as Al, Ti, Ni, Cu, Zr, and their alloys.

1.2 Metallic glasses

The first discovery of a metallic glass was Au_4Si and subsequently, many different types of metallic glass alloys have been produced and characterized (Klement *et*

al., 1960; Duwez, 1978; Johnson, 1998). Some of these metallic glasses exhibit desirable properties for industrial applications, such as low magnetic hysteresis losses (Fe or Co based alloy), high mechanical strength (high yield strength and high elastic strain limit), and high corrosion resistance relative to crystalline alloys with the same composition (Duwez, 1978). However, practical applications have been limited by the high cooling rate (10^5-10^6 K/s) required to form the glass and the difficulty of making bulk (millimeter scale) sized samples (Johnson, 1998).

Recently, new generations of alloys capable of forming a bulk metallic glass (BMG) have been developed by Peker and Johnson (1993). The first family of BMG's have compositions $Zr_{41.2}Ti_{13.8}Cu_{12.5}Ni_{10.0}Be_{22.5}$ (Vitreloy 1) and form metallic glasses with critical cooling rates of only 1 K/s-sufficient to suppress crystallization (Kim *et al.*, 1994). Thus Vitreloy 1 has been used to form fully glassy rods with diameters of 5 to 10 cm (Johnson, 1998).

The discovery of these new generations of BMG's was guided by qualitative reasoning regarding the relative melting and crystallization temperatures of various phases. Earlier, Turnbull predicted that the homogeneous nucleation of crystals becomes very sluggish as the reduced glass transition temperature ($T_r=T_g/T_m$) increases (Turnbull, 1969). This is called *Turnbull's criterion*, which is still one of the best rules of thumb for predicting the glass forming ability of any liquid. Another thermodynamically interesting rule of thumb is the T_0 criterion of glass formation (Baker, 1971; Massalski, 1981). The T_0 temperature is the temperature at which the free energies of the liquid and crystalline phase become identical. The T_0 line can be obtained by connecting the T_0 points at different concentrations (x). This criterion states that glass formation is only possible if

both $T_0(x)$ lines of terminal solid solutions plunge deep enough to cross the $T_g(x)$ lines (Fig. 1-3).

In addition to the alloy development and characterization, modification and modeling mechanical properties have been actively studied in the field of metallic glass research. Even though favorable properties, such as high yield strength and high elastic limit, make metallic glasses a good candidate for engineering materials, the unique catastrophic failure mechanism, due to the formation of shear bands, imposes a challenge. The localization of shear is associated with the absence of strain hardening (work hardening) mechanisms, possible strain softening mechanisms, and thermal softening during adiabatic heating of the material (Johnson, 1998). In an effort to overcome the catastrophic failure mechanism, recent efforts have focused on fabrication of metallic glasses composites, either by direct introduction of crystalline reinforcements into the glass matrix (Choi-Yim, 1999) or by inducing the growth of ductile crystalline phase in the glass matrix (Kim, 2001).

1.3 Phase transitions

When a liquid is cooled and becomes a solid, two kinds of solidification may occur: crystallization or glass transition. Crystallization is commonly observed when a liquid is cooled with a low cooling rate and is characterized by a sharp discontinuity in volume and energy as a function of temperature (Fig. 1-1. path $2 \rightarrow 1$). This is characteristic of a first-order phase transition, defined by discontinuous first derivatives of the Gibbs free energy (*dG/dT* or *dG/dP*) at the transition point (Fig. 1-2(a)). When a

solid melts, this is also a first-order phase transition. At equilibrium, melting and crystallization will occur at the same temperature.

When the cooling rate is sufficiently high, a liquid can bypass crystallization and becomes glass (Fig. 1-1. path 2→3). By definition, a glass is a non-crystalline (amorphous) solid lacking long-range periodicity of the atomic arrangement. Glass transition is homogeneous and occurs over a narrow temperature range near the glass transition temperature (T_g). At T_g, there is no discontinuity in volume but $V(T)$ acquires a small slope (similar to that of a crystal), characteristic of the low thermal expansion of a solid. The continuous change in volume and energy around the glass transition point is similar to a second-order phase transition (Fig. 1-2(b)), defined by discontinuous second derivatives of the Gibbs free energy (d^2G/dT^2 or d^2G/dP^2). In spite of the similarity, the glass transition is not a true thermodynamic phase transition. The glass transition is generally associated with broken ergodicity on the time scale of experimental observation. Thus, the phase space of the glass appears to be smaller than the corresponding liquid.

Many theories for the glass transition have been proposed. The two most studied theories are the free volume theory (Cohen and Turnbull, 1959; Turnbull and Cohen, 1961, 1970; Cohen and Grest, 1979, 1981) and the mode coupling theory (Bengtzelius *et al.*, 1984; Leutheusser, 1984; Gotze and Sjogren, 1992). The former explains the glass transition from a thermodynamic viewpoint and the latter from a dynamic viewpoint.

Free volume theory states that the glass transition occurs when the volume available for atomic motion (the free volume), becomes less than a critical value. At high temperature, sufficient free volume is present to facilitate the configuraional

rearrangements of atoms. However, as the temperature decreases, the available free volume decreases along with the total volume of the system. At some point, the free volume is reduced to a critical level, below which the configuraional rearrangement of atoms becomes impossible. This is the glass state and the temperature at which this happens is T_g.

Mode coupling theory describes the glass transition as a transition from ergodic to nonerogic behavior in the relaxation dynamics, which are solely governed by density fluctuations. This theory predicts that there exists two major relaxation modes, the so-called α relaxation and β relaxation processes. α relaxation is associated with the exploration of deep configurational energy minima and β relaxation is associated with the exploration of local minima in the vicinity of a given deep configurational minimum (Stillinger, 1995). Therefore, at high temperatures, α and β relaxation modes become indistinguishable. However, as the temperature decreases, the α relaxation slows down and shows a singularity at $T=T_c$, while the β relaxation remains finite. T_c is the mode coupling temperature and is considered by mode coupling theory to be the ideal glass transition temperature.

1.4 Molecular dynamics simulation

Molecular dynamics (MD) is a useful technique for obtaining macroscopic properties of a system by calculating the Newtonian dynamics of individual atoms or molecules. The dynamics describe how atomic coordinates r^N and momenta p^N change with time t and this phase space information $\{r^N(t), p^N(t)\}$ is referred to as the trajectories of the system. To generate the trajectories, the initial coordinates and momenta are assigned to the particles. Then, their subsequent trajectories are calculated by numerical

integration of the classical Newtonian or Hamilton's equations of motion. Observable properties of the system, such as temperature, pressure and volume, are then obtained as time averages over the trajectories.

Due to limitations in computational power, MD simulations are usually performed on small systems containing several hundred to a few thousand atoms. Such small systems have high surface to volume ratio, making surface effects important. In simulations where surface effects are not of interest, such as bulk system simulations, surface effects can be removed by using periodic boundary conditions (PBC). Under PBC, the system is composed of a single unit cell, which is replicated throughout space to form an infinite lattice. PBC removes surface effects but introduces artificial periodicity. To eliminate effects from self-interactions, the primary cell dimension L should be larger than twice the atomic interaction range. This makes it impossible to simulate long-range phenomena, where the range of critical fluctuations is macroscopic, for example, when a liquid is close to the gas-liquid critical point. Despite this limitation, it has been shown that PBC have little effect on equilibrium thermodynamic properties and structures of fluids far form the critical point (Pratt and Haan, 1981a, b). In addition to the size limitations, MD simulations are confined to short time scales. Considering that one time step in a MD simulation is typically 10^{-15} s (1 fs), it is not practical to study long-lived phenomena, roughly, those requiring more than 10^{-9} s (1 ns). To assure that the phenomenon of interest can be studied by MD, it is important to estimate the necessary relaxation time.

In the following sections, the MD simulation methods are explained. Also, various physical properties that can be obtained from MD simulations are introduced.

1.4.1 Molecular dynamics methods

In a conventional molecular dynamics simulation, the equations of motion are solved numerically while keeping the number of atoms N and volume V of the system constant. In this case, the energy E and momentum p are conserved because there are no external perturbations. In classical thermodynamics, this is referred to as an isolated system. While an isolated system is easy to simulate using molecular dynamics techniques, it is rarely encountered in real experiments. Hence, the conventional equations of motion need to be extended to describe experimentally interesting conditions, such as constant temperature T or constant pressure P.

To extend the equations of motion (Hamiltonian formulation), it is useful to define an ensemble. Ensemble is a collection of all possible microstates that has the same macroscopic properties of a thermodynamic system in which we are interested. Depending on the experimental condition of interests, a relevant ensemble should be chosen. For example, an isolated system and a closed isothermal system correspond to the microcanonical (constant N, V and E) and canonical (constant N, V and T) ensemble, respectively.

While there is no well-defined way to extend the Hamiltonian formulation, a successful approach has been to introduce additional degrees of freedom (Andersen, 1980). Andersen used V as an additional degree of freedom to achieve constant enthalpy and constant pressure (*HPN*) conditions. Subsequently, Parinello and Rahman generalized Andersen's formula by allowing fluctuations in shape h (Parrinello and Rahman, 1981). By allowing fluctuations in shape (or equivalently, symmetry) and

volume, the stress and strain tensors were calculated to achieve the constant enthalpy and constant thermodynamic tension (*HtN*) condition. This method is especially useful to study of structural phase transitions and the mechanical properties of a crystalline solid, where symmetry is important. In practice, the constant temperature condition is more frequently used than the constant enthalpy condition in real experiments. Therefore, there was incentive to develop methods to generate ensembles under the condition of constant temperature. The most convenient one is introduced by Nose (Nose, 1984) and later generalized by Hoover (Hoover, 1985). In this method, the constant temperature condition is achieved by coupling the momenta of the atoms to an external heat bath. Soon after the introduction of Nose's ideas, Ray and Rahman (Ray and Rahman, 1984, 1985) combined Nose's ideas with the Parrinello-Rahman theory to achieve the constant temperature and constant thermodynamic tension (*TtN*) condition. Much of the work in this thesis is based on Ray and Rahman's single Hamiltonian formulation, which can generate *EhN*, *ThN*, *HtN*, and *TtN* ensembles.

1.4.2 Hamiltonian formulation

The Hamiltonian for the *TtN* ensemble is expressed as:

$$H(s,p,h,\Pi,f,P)=\sum_i \frac{\tilde{p}_i G^{-1} p_i}{2m_i f^2}+U+\frac{Tr(\tilde{\Pi}\Pi)}{2W}+V_0 Tr(te)+\frac{P^2}{2M}+(3N+1)K_B T_0 \ln(f) \tag{1-1}$$

Here, (s_i,p_i) are the scaled coordinates and conjugate momentum of particle *i*. *(h,P)* are the shape and momentum tensor of the primary MD cell. (*f*, *P*) are the Nose mass scaling variable and its conjugate momentum. The metric tensor *G* is defined by $G=\tilde{h}h$ and *U*

is the potential energy. The parameters *W*, called "piston mass" and *M*, called "thermal inertia," are introduced so that *h* and *f* satisfy dynamical equations. V_0 is the reference volume, defined by $V_0=det(h_0)$, where h_0 is the reference shape tensor at zero tension. T_0 is the thermal reservoir temperature and *e* is the strain matrix which is defined by

$$e = (\tilde{h}_0^{-1} G h_0^{-1} - 1)/2, \tag{1-2}$$

where the tilde indicates matrix transpose.

In this Hamiltonian formulation, the particle position and momentum (r_i, p_i) are related to the scaled particle variables (s_i,p_i) by $r_i = hs_i$ and $p_i = \tilde{h}^{-1} p_i / f$, where s_i range from 0 to1. Therefore, the kinetic energy *(KE)* is represented by the first term in Hamiltonian and the second term is internal energy *(U)*. The third and fourth terms are related to the elastic energy of the system. Finally, the fifth and sixth terms are kinetic term and potential term for the Nose mass scaling variable *f*, to achieve constant temperature dynamics.

Using the Hamiltonian Eq. 1-1, equation of motion can be derived as:

$$m_i f^2 \ddot{s}_{ia} = -\sum_{j \neq i} \frac{(\partial U / \partial r_{ij}) s_{ija}}{r_{ij}} - m_i (f^2 G^{-1} \dot{G} + 2 f \dot{f}) s_{ia} \tag{1-3}$$

$$W \ddot{h}_{ab} = P_{ab} V \tilde{h}^{-1} - h V_0 h_0^{-1} t \tilde{h}_0^{-1} \tag{1-4}$$

$$M \ddot{f} = \frac{2KE}{f} - \frac{(3N+1) k_B T_0}{f} \tag{1-5}$$

Here, subscript *a* and *b* represent *x*,*y*, and *z* direction. P_{ab} is the microscopic stress tensor can be expressed as:

$$P_{ab} = \frac{1}{V} \sum_i \frac{p_{ia} p_{ib}}{m_i} - \sum_{i<j} \frac{1}{r_{ij}} \left(\frac{\partial U}{\partial r_{ij}} \right) r_{ija} r_{ijb} \tag{1-6}$$

Therefore, the Hamiltonian for *TtN* dynamics requires the solutions of 3*N*+9+1 equation of motions. *N* is the number of atoms with 3 degrees of freedom, *h* matrix has 9 independent components, and one more degree of motion of *f*.

Subsequently, Hamiltonians for *EhN*, *ThN*, and *HtN* dynamics can be obtained from the Hamiltonian for *TtN* dynamics with constraints (Ray and Rahman, 1984, 1985). If the Nose variable is constant as *f*=1 and the shape matrix *h* is constant, the Hamiltonian for *TtN* dynamics reduces to the Hamiltonian for the *EhN* dynamics. If only *h* is constant, the Hamiltonian for the *ThN* dynamics is obtained. If only the Nose variable is constant as *f=1*, the Hamiltonian for the *HtN* dynamics is obtained.

1.4.3 Determination of thermodynamic properties

Provided any measurable property *A* in terms of the phase space trajectory $\{\mathbf{r}^N(t),\mathbf{p}^N(t)\}$ of any ensemble, the experimentally observable macroscopic property can be expressed as the time average:

$$< A >= \frac{1}{t}\int_{t_0}^{t_0+t} A(\mathbf{r}^N(t),\mathbf{p}^N(t))dt \qquad (1\text{-}7)$$

In general, τ should be long enough to include several multiples of the relaxation time for the corresponding property. Using Eq. 1-7, the simple thermodynamic properties such as the potential energy *U*, the kinetic energy *KE*, the temperature *T*, the volume *V* and the pressure *P* can be calculated by averaging the corresponding properties over a time period. However, several thermodynamic properties cannot be determined in the same way, such as the entropy *S* and properties related to entropy (the Helmholtz free energy *F*, the Gibbs free energy *G*, and the chemical potential μ). This is because these

properties are not a function of the phase space trajectory $\{\mathbf{r}^N(t),\mathbf{p}^N(t)\}$, rather they are a function of the accessible phase space volume for the system. Separate techniques are required to evaluate such thermodynamic quantities from MD (Frenkel, 1996).

Other thermodynamic properties, such as heat capacities and isothermal compressibility, are the thermodynamic response functions, which are derivatives of the simple thermodynamic quantities. The response functions capture the response of simple thermodynamic quantities to changes in measurable quantities, typically either the pressure or temperature. Since they are derivative quantities, they are analytically related to the thermodynamic fluctuations via statistical mechanics. Thus,

$$C_V = \left(\frac{\partial E}{\partial T}\right)_V = \frac{\left\langle (dE)^2 \right\rangle_{NVT}}{k_B T^2} \qquad \text{(isometric heat capacity)} \qquad (1\text{-}8)$$

$$C_P = \left(\frac{\partial H}{\partial T}\right)_P = \frac{\left\langle (dH)^2 \right\rangle_{NPT}}{k_B T^2} \qquad \text{(isobaric heat capacity)} \qquad (1\text{-}9)$$

$$b_T = \frac{-1}{V}\left(\frac{\partial V}{\partial P}\right)_T = \frac{\left\langle (dV)^2 \right\rangle_{NPT}}{k_B T V} \qquad \text{(isothermal compressibility)} \qquad (1\text{-}10)$$

Here, dA is the fluctuation of the dynamic value A about its average value $\langle A \rangle$

$$dA = A - \langle A \rangle \qquad (1\text{-}11)$$

Therefore, $\langle (dA)^2 \rangle$ is the mean square fluctuation.

$$\langle (dA)^2 \rangle = \langle (A - \langle A \rangle)^2 \rangle = \langle A^2 \rangle - \langle A \rangle^2 \qquad (1\text{-}12)$$

All remaining response functions can be evaluated using the thermodynamic fluctuations combined with classical thermodynamic relations (Haile, 1997).

1.4.4 Determination of structural properties

To describe structural properties, a statistical description of relative atomic configurations, such as radial distribution function (RDF or *g(r)*), is commonly used. The *g(r)* is particularly useful because it can be obtained experimentally by applying a Fourier transform to X-ray diffraction data. By definition, *g(r)* is the probability of finding a pair of atoms separated by a distance *r*, relative to the probability for a random distribution at the same density. Eq. 1-13 shows the mathematical expression of *g(r)*.

$$g(r) = \frac{V}{N^2} < \sum_{i}^{N} \sum_{j \neq i}^{N} d(r - r_{ij}) > \tag{1-13}$$

Here r_{ij} is the distance between atom i and j, $d(x)$ is the Dirac delta function, and the angular brackets represent the time average.

Crystalline solids are structurally well defined. Therefore, in this case, *g(r)* for crystalline solids are characterized by sharp peaks around each lattice site and the width of peak is correlated to the temperature of the system. A typical *g(r)* for an FCC crystalline solid is shown in Fig. 1-4. For liquids, *g(r)* is characterized by broad peaks that represent a shell of neighbors and an asymptotic value of $g(r)=1$ for large r. *g(r)* is also useful in characterizing the structure of glasses (Finney, 1977). In glasses, *g(r)* shows a unique second peak split and this is indicative of amorphous atomic packing.

1.4.5 Determination of transport properties

Transport properties are responses of a system that has not reached equilibrium. For example, diffusion is the atomic motion due to the concentration gradient and its macroscopic description is known as Fick's law. In this sense, transport properties can be calculated by non-equilibrium MD methods only. In non-equilibrium MD, an external force is applied to the system to establish the non-equilibrium situations of interest, and

the system's response to the force is then determined from the simulation. However, the conventional MD (equilibrium MD) also can be used to obtain transport properties by measuring microscopic fluctuations in the system. This is achieved by calculating time correlation functions *C(t)*, which captures how a dynamic quantity *A(t)* is related to the other dynamic quantity *B(t)*.

$$C(t) = \lim_{t \to \infty} \frac{1}{t} \int_0^t A(t_0) B(t_0 + t) dt \qquad (1\text{-}14)$$

Some examples of the relation between microscopic fluctuations with transport properties are shown as below.

$$D = \frac{1}{3} \int_0^\infty dt < v_i(t) \cdot v_i(0) > \qquad \text{(diffusion coefficient)} \qquad (1\text{-}15)$$

$$h_S = \frac{V}{k_B T} \int_0^\infty dt \; < P_{ab}(t) P_{ab}(0) > \qquad \text{(shear viscosity)} \qquad (1\text{-}16)$$

$$h_V = \frac{V}{9 k_B T} \sum_{ab} \int_0^\infty dt \; < dP_{aa}(t) dP_{bb}(0) > = \frac{V}{k_B T} \int_0^\infty dt \; < dP(t) dP(0) >$$

(bulk viscosity) (1-17)

Here, $v_i(t)$ is the velocity of an atom *i*, $P_{ab}(t)$ is off diagonal ($a \neq b$) term of the pressure tensor, and $P_{aa}(t)$ or $P_{bb}(t)$ are diagonal terms in the pressure tensor.

1.4.6 Force-field and parameters

To simulate material properties and processes using MD methods, a functional form for the interatomic potential $U(r^N)$ must be chosen. Many studies of metallic glasses have used pair potentials such as Lennard-Jones potential (Woodcock *et al.*, 1976; Abraham, 1980; Fox and Andersen, 1984; Jonsson and Andersen, 1988; Wahnstrom,

1991; Li and Johnson, 1993; Kob, 1999). Such simulations provide an important theoretical means to study the properties of glasses, including the nature of the glass transition. However, pair potentials have intrinsic limitations when applied to metallic systems. For example, systems described with pair potentials always satisfy the Cauchy relation $C_{12}=C_{44}$ between elastic constants, whereas metallic systems typically strongly disobey the Cauchy relation (Thomas, 1971). In addition, pair potentials cannot describe the volume dependency of potential energy in metallic systems, which is known to be important in metallic systems (Heine, 1970). Thus, we believe that it is essential to include many-body interactions in studying the phase behavior of metals and metal alloys.

In this thesis, the Sutton-Chen (SC) many-body potential is used, which has a simple power law form and relatively long-range character (Sutton and Chen, 1990). The SC many-body potential has the form

$$U_{tot} = \sum_i U_i = \sum_i \left[\frac{1}{2} \sum_{j \neq i} \varepsilon_{ij} V(r_{ij}) - c_i \varepsilon_{ii} \rho_i^{1/2} \right], \tag{1-18}$$

$$\text{where } V(r_{ij}) = \left(\frac{a_{ij}}{r_{ij}} \right)^n \tag{1-19}$$

$$\text{and } \rho_i = \sum_{j \neq i} f(r_{ij}) = \sum_{j \neq i} \left(\frac{a_{ij}}{r_{ij}} \right)^m . \tag{1-20}$$

r_{ij} is the distance between atom i and j. $V(r_{ij})$ is a repulsive pair potential between atoms i and j, accounting for the Pauli repulsion between the core electrons. The cohesion associated with atom i is captured in a local energy density ρ_i. ε sets the overall energy

scale and c_i is a dimensionless parameter scaling the attractive term. a is a length parameter leading to a dimensionless form for V and r.

The force-field parameters for the SC potential were optimized to reproduce experimental properties such as density, cohesive energy, bulk modulus, elastic constants, phonon dispersion, vacancy formation energy, and surface energy (Kimura, 1998). In calculating these properties, quantum corrections were included, leading to the quantum Sutton-Chen, or Q-SC force field (Yoshitaka Kimura, 1998). The Q-SC parameter sets for Cu is presented in Table 1 and has been employed successfully in earlier studies (Cagin *et al.*, 1999; Ikeda *et al.*, 1999; Qi *et al.*, 1999, 2002).

For alloys, we use the following combination rules to describe the interaction between different types of atoms:

$$e_{ij} = \sqrt{e_{ii} e_{jj}}\,, \tag{1-21}$$

$$n_{ij} = \frac{1}{2}(n_i + n_j)\,, \tag{1-22}$$

$$m_{ij} = \frac{1}{2}(m_i + m_j)\,, \tag{1-23}$$

$$\text{and } a_{ij} = \sqrt{a_{ii} a_{jj}}\,. \tag{1-24}$$

These combination rules describe the concentration dependencies of the lattice parameters and elastic constants of simple alloy systems with good accuracy (Rafiitabar and Sutton, 1991).

References

Abraham, F.F. (1980). Isothermal-Isobaric Computer-Simulation of the Supercooled-Liquid-Glass Transition Region - Is the Short-Range Order in the Amorphous Solid Fcc. J. Chem. Phys. *72*, 359-365.

Andersen, H.C. (1980). Molecular-Dynamics Simulations at Constant Pressure and-or Temperature. J. Chem. Phys. *72*, 2384-2393.

Anderson, P.W. (1995). Through the Glass Lightly. Science *267*, 1615.

Baker, J.C.a.C., J. W. (1971). Thermodynamics of solidification. ASM, Metals Park: Ohio.

Bengtzelius, U., Gotze, W., and Sjolander, A. (1984). Dynamics of Supercooled Liquids and the Glass-Transition. Journal of Physics C-Solid State Physics *17*, 5915-5934.

Cagin, T., Dereli, G., Uludogan, M., and Tomak, M. (1999). Thermal and mechanical properties of some fcc transition metals. Phys. Rev. B *59*, 3468-3473.

Choi-Yim, H. (1999). Synthesis and Characterization of Bulk Metallic Glass Matrix Composites, California Institute of Technology.

Cohen, M.H., and Grest, G.S. (1979). Liquid-Glass Transition, a Free-Volume Approach. Phys. Rev. B *20*, 1077-1098.

Cohen, M.H., and Grest, G.S. (1981). A New Free-Volume Theory of the Glass-Transition. Ann.NY Acad.Sci. *371*, 199-209.

Cohen, M.H., and Turnbull, D. (1959). Molecular Transport in Liquids and Glasses. J. Chem. Phys. *31*, 1164-1169.

Duwez, P. (ed.) (1978). Metallic glasses. American Society for Metals.

Finney, J.L. (1977). Modeling Structures of Amorphous Metals and Alloys. Nature *266*, 309-314.

Fox, J.R., and Andersen, H.C. (1984). Molecular-Dynamics Simulations of a Supercooled Monatomic Liquid and Glass. J. Phys. Chem. *88*, 4019-4027.

Frenkel, D.a.S., B. (1996). Understanding molecular simulation. Academic press.

Gotze, W., and Sjogren, L. (1992). Relaxation Processes in Supercooled Liquids. Rep. Prog. Phys. *55*, 241-376.

Haile, J.M. (1997). Molecular dynamics simulation. A Wiley-Interscience Publication.

Heine, V.a.W., D. (1970). Solid state physics. In: Solid state physics, vol. 24, ed. E.H.a.T. D., New York: Academic press, 249-463.

Hoover, W.G. (1985). Canonical Dynamics - Equilibrium Phase-Space Distributions. Phys. Rev. A *31*, 1695-1697.

Ikeda, H., Qi, Y., Cagin, T., Samwer, K., Johnson, W.L., and Goddard, W.A. (1999). Strain Rate Induced Amorphization in Metallic Nanowires. Phys. Rev. Lett. *82*, 2900-2903.

Johnson, W.L. (1998). Bulk glass-forming metallic alloys: science and technology. In: Mat. Res. Soc. Symp. Proc., vol. 554, ed. A.I.a.C.T.L. William L. Johnson, Boston, MA: Mateirals Research Society, 311.

Jonsson, H., and Andersen, H.C. (1988). Icosahedral Ordering in the Lennard-Jones Liquid and Glass. Phys. Rev. Lett. *60*, 2295-2298.

Kim, C.P. (2001). Ductile Phase Reinforced Bulk Metallic Glass Composites Formed by Chemical Partitioning, Calfornia Institute of Technology.

Kim, Y.J., Busch, R., Johnson, W.L., Rulison, A.J., and Rhim, W.K. (1994). Metallic-Glass Formation in Highly Undercooled Zr41.2ti13.8cu12.5ni10.0be22.5 During Containerless Electrostatic Levitation Processing. Appl. Phys. Lett. *65*, 2136-2138.

Kimura, Y., Cagin, T., Qi, Y., and Goddard III, W. A. (1998). The Quantum Sutton-Chen Many-Body Potential for Properties of fcc Metals.

Klement, W., Willens, R.H., and Duwez, P. (1960). Non-Crystalline Structure in Solidified Gold-Silicon Alloys. Nature *187*, 869-870.

Kob, W. (1999). Computer simulations of supercooled liquids and glasses. J. Phys.-Condes. Matter *11*, R85-R115.

Lee, H.-J., Qi, Y., Cagin, T. C., Johnson, W. L., and Goddard III, W. A. (2000). Molecular Dynamics Simulations of Supercooled Liquid Metals and Glasses. Mat. Res. Soc. Symp., Boston, *644*, L2.3.1.

Leutheusser, E. (1984). Dynamical Model of the Liquid-Glass Transition. Phys. Rev. A *29*, 2765-2773.

Li, M., and Johnson, W.L. (1993). Instability of Metastable Solid-Solutions and Crystal to Glass- Transition. Phys. Rev. Lett. *70*, 1120-1123.

Massalski, T.B. (1981). The 4th international conference on rapidly quenched metals.

Nose, S. (1984). A Unified Formulation of the Constant Temperature Molecular-Dynamics Methods. J. Chem. Phys. *81*, 511-519.

Parrinello, M., and Rahman, A. (1981). Polymorphic Transitions in Single-Crystals - a New Molecular- Dynamics Method. J. Appl. Phys. *52*, 7182-7190.

Peker, A., and Johnson, W.L. (1993). A Highly Processable Metallic-Glass - Zr41.2ti13.8cu12.5ni10.0be22.5. Appl. Phys. Lett. *63*, 2342-2344.

Pratt, L.R., and Haan, S.W. (1981a). Effects of Periodic Boundary-Conditions on Equilibrium Properties of Computer-Simulated Fluids .1. Theory. J. Chem. Phys. *74*, 1864-1872.

Pratt, L.R., and Haan, S.W. (1981b). Effects of Periodic Boundary-Conditions on Equilibrium Properties of Computer-Simulated Fluids .2. Application to Simple Liquids. J. Chem. Phys. *74*, 1873-1876.

Qi, Y., Cagin, T., Kimura, Y., and Goddard, W.A. (1999). Molecular Dynamics Simulations of Glass Formation and Crystallization in Binary Liquid Metals: Cu-Ag and Cu-Ni. Phys. Rev. B *59*, 3527-3533.

Qi, Y., Cagin, T., Kimura, Y., and Goddard, W.A. (2002). Viscosities of Liquid Metal Alloys from Nonequilibrium Molecular Dynamics. J. Comput-Aided Mater. Des. *8*, 233-243.

Rafiitabar, H., and Sutton, A.P. (1991). Long-Range Finnis-Sinclair Potentials for Fcc Metallic Alloys. Philos. Mag. Lett. *63*, 217-224.

Ray, J.R., and Rahman, A. (1984). Statistical Ensembles and Molecular-Dynamics Studies of Anisotropic Solids. J. Chem. Phys. *80*, 4423-4428.

Ray, J.R., and Rahman, A. (1985). Statistical Ensembles and Molecular-Dynamics Studies of Anisotropic Solids .2. J. Chem. Phys. *82*, 4243-4247.

Stillinger, F.H. (1995). A Topographic View of Supercooled Liquids and Glass-Formation. Science *267*, 1935-1939.

Sutton, A.P., and Chen, J. (1990). Long-Range Finnis Sinclair Potentials. Philos. Mag. Lett. *61*, 139-146.

Thomas, J.F. (1971). Failure of Cauchy Relation in Cubic Metals. Scripta Metallurgica *5*, 787-&.

Turnbull, D. (1969). Under What Conditions Can a Glass Be Formed. Contemp. Phys. *10*, 473-&.

Turnbull, D., and Cohen, M.H. (1961). Free-Volume Model of Amorphous Phase - Glass Transition. J. Chem. Phys. *34*, 120-&.

Turnbull, D., and Cohen, M.H. (1970). On Free-Volume Model of Liquid-Glass Transition. J. Chem. Phys. *52*, 3038-&.

Wahnstrom, G. (1991). Molecular-Dynamics Study of a Supercooled 2-Component Lennard- Jones System. Phys. Rev. A *44*, 3752-3764.

Woodcock, L.V., Angell, C.A., and Cheeseman, P. (1976). Molecular-Dynamics Studies of Vitreous State - Simple Ionic Systems and Silica. J. Chem. Phys. *65*, 1565-1577.

Yoshitaka Kimura, T.C., Yue Qi and William A. Goddard III. (1998). The Quantum Sutton-Chen Many-Body Potential for Properties of fcc Metals.

Zallen, R. (1998). The Physics of Amorphous Solids. A Wiley-Interscience Publication.

Table 1-1.
(a) Parameters for the quantum Sutton-Chen (Q-SC) many-body potential for Cu (Kimura, 1998).

	ε(meV)	c	m	n	a (A)
Cu	5.7921	84.843	5	10	3.603

(b) The lattice constant a, cohesive energy E_{coh}, elastic constants C_{ij}, and bulk modulus B calculated using the Q-SC force field parameters for TtN molecular dynamics calculations. Unless otherwise indicated, the computed values are for the minimized structures. These values are compared to experimental (Exp) values at T=0K, unless otherwise indicated (Kimura, 1998).

	a(T=0K) [A]	a(T=300K) [A]	E_{coh} [eV/atom]	C_{11} [GPa]	C_{12} [GPa]	C_{44} [GPa]	B [GPa]
Exp	3.603	3.615	3.49	176.2	124.9	81.8	142.0
Q-SC	3.603	3.622	3.49	164.5	114.5	71.0	131.2

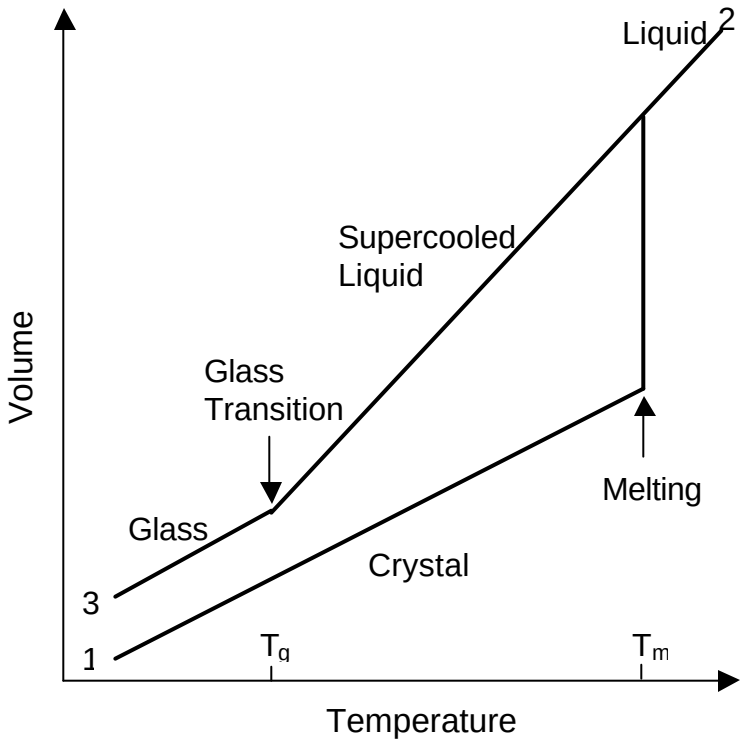

Figure 1-1. A schematic illustration of volume as a function of temperature, demonstrating various phase behaviors. Upon heating (1→2), a crystalline solid melts at the melting temperature T_m. Upon cooling, with sufficiently low cooling rate (2→1), liquid crystallizes at T_m. However, at sufficiently high cooling rate (2→3), a liquid may solidify into a glass in a narrow temperature range near the glass transition temperature T_g.

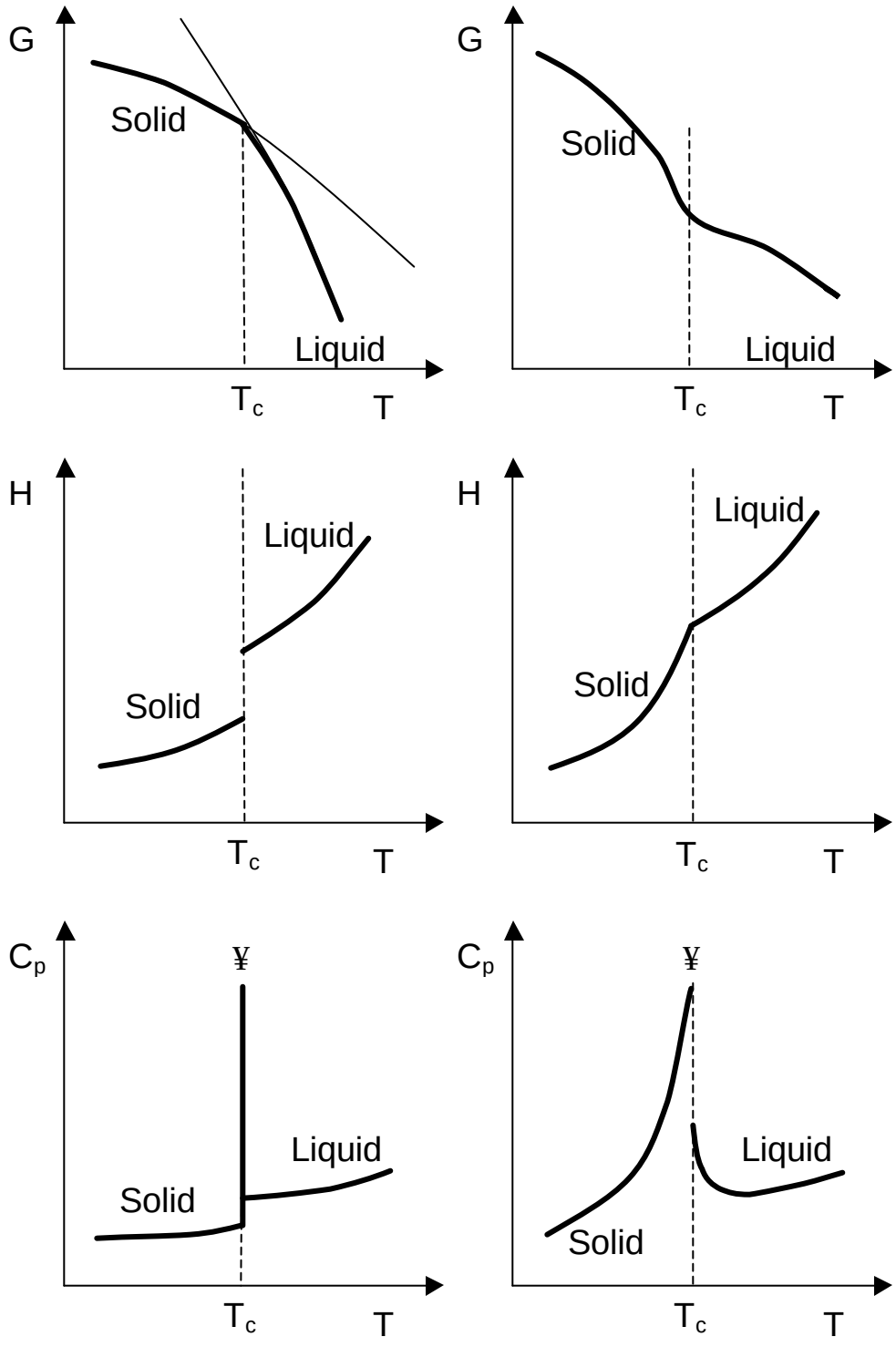

Figure 1-2. Thermodynamic characteristics of (a) first-order and (b) second-order phase transformations (reproduced from (Porter and Easterling, 1981)).

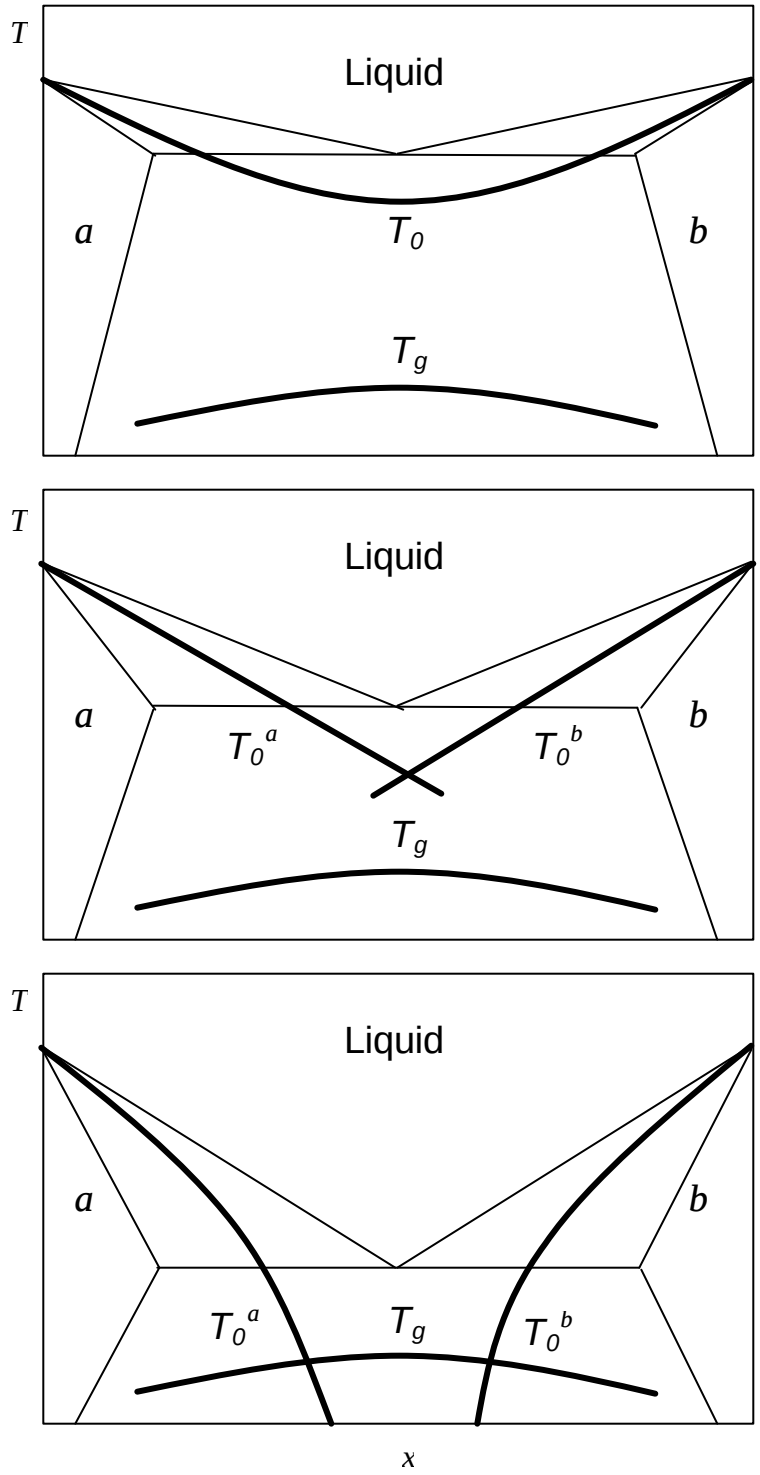

Figure 1-3. Three possible T_0 curves (polymorphic melting curves) for simple eutectic systems. From top to bottom the glass forming ability increases (reproduced from (Peker, 1994)).

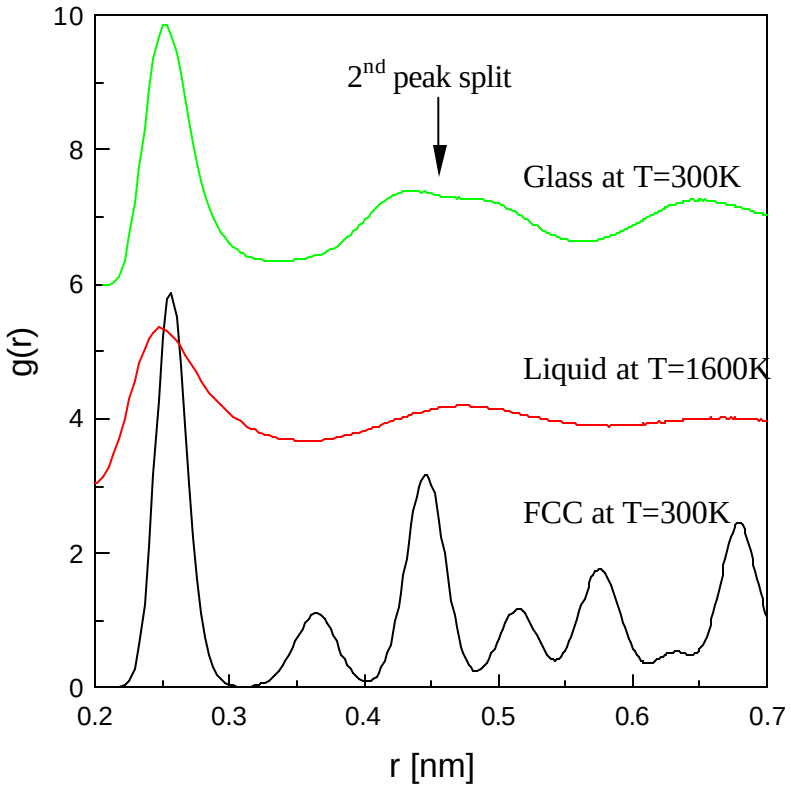

Figure 1-4. The radial distribution functions *g(r)* of a FCC, liquid, and glass system (from bottom to top). The FCC *g(r)* peaks are at s, $\sqrt{2}s$, $\sqrt{3}s$, $2s$, $\sqrt{5}s$, $\sqrt{6}s$, $\sqrt{7}s$, where s is the first nearest neighbor distance. The liquid *g(r)* shows broad peaks that represent a shell of neighbors and an asymptotic value of *g(r)*=1 for large *r*. The glass *g(r)* shows a splitting in a second peak, which is a characteristic of amorphous atomic packing.